35th Annual International Conference of the IEEE EMBS
Osaka, Japan, 3 - 7 July, 2013

Subspace Method Decomposition and Identification of the Parallel-cascade Model of Ankle Joint Stiffness: Theory and Simulation

Kian Jalaleddini, Student Member, IEEE and Robert E. Kearney, Fellow, IEEE

***Abstract*— This paper describes a state-space representation of the parallel-cascade model of ankle joint stiffness whose parameters are directly related to the underlying dynamics of the system. It then proposes a two step subspace method to identify this model. In the first step, the intrinsic stiffness is estimated using proper orthogonal projections. In the second step, the reflexive pathway is estimated by iterating between estimating its nonlinear and linear components. The identified models can be easily converted to continuous-time for physiological interpretation. Monte-Carlo studies using simulated data which replicate closely the experimental conditions, were used to compare the performance of the new method with the previous parallel-cascade, and subspace methods. The new method is more robust to noise and is guaranteed to converge.**

I. INTRODUCTION

Joint stiffness defines the dynamic relation between the position of the joint and the torque acting about it [1]. It plays an important role in the control of posture and movement [2]. Consequently, its identification is important to the study of posture and movement [3], [4], [1]. Joint stiffness consists of two components: (a) an intrinsic component that is due to the mechanical properties of the limb, joint and muscle; (b) a reflex component which originates from the stretch reflex arc [4].

Fig. 1 shows a small signal, parallel-cascade model for joint stiffness. In this model, the intrinsic component has a linear representation and the reflex component has a differentiator followed by a delay and a Hammerstein system (i.e. the cascade of a static nonlinear and dynamic linear blocks). Total joint torque is the summation of the intrinsic and reflex torques.

The parallel-cascade method proposed in [1] separates and identifies the intrinsic and reflex components using a non-parametric approach by iterating between the intrinsic and reflex pathways estimations. Our laboratory has extensively used the parallel-cascade method to study stiffness in both control and stroke patients [4], [5]. A real time version of the method was also implemented and used to show that subjects could voluntarily modulate their stiffness [6]. Despite its utility, the parallel-cascade method has some shortcomings. First, the iteration which is central to the method may not always converge; especially when the reflex contribution is small or the *signal to noise ratio* SNR is low. Second, its methods are correlation-based and will fail for measurements made in closed loop - as will be the case when the joint interacts with a compliant load [7], [3].

K. Jalaleddini is with the Department of Biomedical Engineering, McGill University, 3775 University, Montréal, Québec H3A 2B4, Canada. seyed.jalaleddini@mail.mcgill.ca.

R. E. Kearney is with the Department of Biomedical Engineering, McGill University, 3775 University, Montréal, Québec H3A 2B4, Canada. kearney@mcgill.ca.

This work has been supported by CIHR, NSERC and FQRNT.

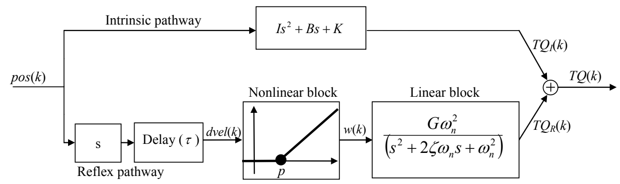

Fig. 1. Parallel-cascade model of ankle joint stiffness [1].

To address these issues, our laboratory developed a state-space model of stiffness and used a subspace method to estimate it [8] . This method required no iteration, gave unbiased results when used with closed-loop data, and produced models that had excellent predictive abilities. However, these models had many parameters, each of which depended on the properties of both the static nonlinear and the linear components in the reflex pathway. This made it difficult to convert the state-space model to the continuous-time model needed to interpret the physiological significance of the results

To address these problems, this paper reformulated the state-space model used in [8] to have parameters there were fewer in number and were directly related to the static nonlinear or linear components of the Hammerstein structure. Consequently, the new identification method estimates all elements of the parallel-cascade model individually so that converting it to a continuous-time model is straightforward. The identification method is also new. The intrinsic pathway is now estimated directly using orthogonal projections. The reflex path elements are then estimated using a Hammerstein identification algorithm [9] with guaranteed convergence.

II. THEORY

A. Formulation

Fig. 1 shows the parallel-cascade model of joint stiffness. The intrinsic stiffness relates the intrinsic torque ($TQ_I(k)$) to the joint position by means of inertial (I), viscous (B) and elastic (K) terms: $\frac{TQ_I}{POS} = Is^2 + Bs + K$.

The reflex pathway differentiates and delays the input position which is then fed to a Hammerstein structure, i.e., cascade of a static nonlinearity followed by a linear system. Approximate the static nonlinearity by a basis expansion:

$$w(k) = \alpha_1 g_1\left(dvel(k)\right) + \cdots + \alpha_n g_n\left(dvel(k)\right) \quad (1)$$

where $w(k)$ is the output of the nonlinearity, $dvel(k)$ is the delayed velocity (the input to the nonlinearity), $g_i(\cdot)$ is the i^{th} basis function and α_i is its coefficient.

Let the following state-space model represent the linear component between $w(k)$ and the reflex torque $TQ_R(k)$:

$$\begin{cases} x_R(k+1) & = A_R x_R(k) + B_R w(k) \\ TQ_R(k) & = C_R x_R(k) + D_R w(k) \end{cases} \tag{2}$$

where $x_R(k)$ is the state vector at time $k \in \{0, \cdots, N-1\}$, and A_R, B_R, C_R and D_R are the state-space matrices. Let the elements of B_R and D_R be:

$$B_R = \begin{bmatrix} b_1 & \cdots & b_m \end{bmatrix}^T \; D_R = [d] \tag{3}$$

Now, the total state-space formulation is [8]:

$$\begin{cases} x(k+1) & = A x_R(k) + BU(k) \\ \tilde{T}Q(k) & = C x_R(k) + DU(k) + v(k) \end{cases} \tag{4}$$

where $\tilde{T}Q(k)$ is the measured torque contaminated with the noise sequence $(v(k))$ and $U(k)$ is a constructed input vector:

$$\begin{aligned} U_R(k) &= \begin{bmatrix} g_1(dvel(k)) & \cdots & g_n(dvel(k)) \end{bmatrix}^T \\ U_I(k) &= \begin{bmatrix} pos(k) & vel(k) & acc(k) \end{bmatrix}^T \\ U(k) &= \begin{bmatrix} U_R^T \; U_I^T \end{bmatrix} \end{aligned} \tag{5}$$

The algorithm described in [8] estimates the state-space matrices A, B, C, D of (4) which provides output prediction. Establishing the mapping from these matrices to the original system requires further analysis of the structure of these matrices.

The A and C matrices are simply the A_R and C_R matrices of the linear block of the reflex stiffness. However, the matrices B and D have the following structure:

$$\begin{aligned} B &= \begin{bmatrix} b_1\alpha_1 & \cdots & b_1\alpha_n & 0 & 0 & 0 \\ \vdots & & \vdots & \vdots & \vdots & \vdots \\ b_m\alpha_1 & \cdots & b_m\alpha_n & 0 & 0 & 0 \end{bmatrix} \\ D &= \begin{bmatrix} d\alpha_1 & \cdots & d\alpha_n & K & B & I \end{bmatrix} \end{aligned} \tag{6}$$

Thus, the estimates of the elements of B and D do not directly specify the structure of the nonlinearity or the linear system. This is because these are combinations of the parameters of the nonlinearity (α_i), the linear elements of the reflex stiffness ($\{b_1, \cdots, b_m, d\}$) and intrinsic stiffness parameters ($\{I, B, K\}$). Consequently, the objective is to develop an identification algorithm that estimates these parameters directly.

B. Identification Algorithm

We will use the *multivariable output error state space* MOESP algorithm with *past input* PI as instrumental variable to estimate the system matrices $\hat{A}$ and $\hat{C}$. This method provides unbiased estimates of these matrices for an additive, arbitrarily colored noise [10].

To identify the remaining system parameters, express the output torque as a least-squares problem [10]:

$$Y = \Psi\theta + V \tag{7}$$

where Ψ is constructed from known elements:

$$\Psi = \begin{bmatrix} 0 & U^T(0) \\ \vdots & \vdots \\ \sum_{\tau=0}^{N-2} U_R^T(\tau) \otimes \hat{C}\hat{A}^{N-2-\tau} & U^T(N-1) \end{bmatrix}$$

and $\otimes$ is the Kronecker product and Y, V and θ are:

$$\begin{aligned} Y &= \begin{bmatrix} \tilde{T}Q(0) & \cdots & \tilde{T}Q(N-1) \end{bmatrix}^T \\ V &= \begin{bmatrix} v(0) & \cdots & v(N-1) \end{bmatrix}^T \\ \theta &= [\, b_1\alpha_1 \;\; \cdots \;\; b_m\alpha_1 \;\; \cdots \;\; b_1\alpha_n \;\; \cdots \;\; b_m\alpha_n \\ & \quad \cdots \;\; d\alpha_1 \;\; \cdots \;\; d\alpha_n \;\; K \;\; B \;\; I \,]^T \end{aligned}$$

Rewrite the data equation (7) by separating the intrinsic and reflex contributions:

$$Y = \Psi_R\theta_R + \Psi_I\theta_I + V \tag{8}$$

where Ψ_I and Ψ_R are:

$$\Psi_R = \begin{bmatrix} 0 & U_R^T(0) \\ \vdots & \vdots \\ \sum_{\tau=0}^{N-2} U_R^T(\tau) \otimes \hat{C}\hat{A}^{N-2-\tau} & U_R^T(N-1) \end{bmatrix} \tag{9}$$

$$\Psi_I = \begin{bmatrix} U_I^T(0) \\ \vdots \\ U_I^T(N-1) \end{bmatrix}, \; \theta_I = \begin{bmatrix} K \\ B \\ I \end{bmatrix}$$

$$\theta_R = \begin{bmatrix} b_1\alpha_1 & \cdots & b_m\alpha_n & d\alpha_1 & \cdots & d\alpha_n \end{bmatrix}^T$$

As the first step, estimate θ_I independently of θ_R by using an orthogonal projection on the column space of Ψ_I and Ψ_R to remove the effects of noise and contributions of θ_R. Using (8), solve for θ_I and θ_R as follows:

$$\hat{\theta}_I = \Psi_I^\dagger (Y - \Psi_R\theta_R) \tag{10}$$

$$\hat{\theta}_R = \Psi_R^\dagger (Y - \Psi_I\theta_I) \tag{11}$$

where $\dagger$ is the pseudo-inverse operator. $\hat{\theta}_R$ and $\hat{\theta}_I$ will be unbiased estimates of θ_R and θ_I given that $v(k)$ is zero-mean. Substitute θ_R in (10) with its estimate (11):

$$\underbrace{\left(I - \Psi_I^\dagger\Psi_R\Psi_R^\dagger\Psi_I\right)}_{H}\theta_I = \Psi_I^\dagger\left(I - \Psi_R\Psi_R^\dagger\right)Y \tag{12}$$

Estimate θ_I as follows [11]:

$$\hat{\theta}_I = H^\dagger\Psi_I^\dagger\left(I - \Psi_R\Psi_R^\dagger\right)Y \tag{13}$$

Once θ_I is estimated, we can remove its contribution to the measured torque to give Y_R, an estimate of the reflex torque:

$$Y_R = Y - \Psi_I\hat{\theta}_I = \Psi_R\theta_R \tag{14}$$

Once an estimate of the reflex torque is available, use the subspace Hammerstein method described in [9] to estimate the matrices $B_R = \{b_1, \cdots, b_m\}$, $D_R = \{d\}$ and the coefficients of the static nonlinearity $\alpha = \{\alpha_1, \cdots, \alpha_n\}$ [9]. The whole method is summarized below:

Algorithm: The algorithm identifies intrinsic and reflex components of the parallel-cascade model of ankle joint stiffness.

1. Record N samples of position input and noisy torque.
2. Construct the input signal U using (5).
3. Use PI-MOESP to estimate the order of the reflex system and the state-space matrices A_R and C_R.
4. Construct regressors Ψ_I and Ψ_R using (9).
5. Estimate elastic, viscous and inertial parameters of the intrinsic path using (13).
6. Estimate Y_R using (14).
7. Estimate parameters of B_R, D_R and $\{\alpha_1, \cdots, \alpha_n\}$ using the iterative Hammerstein method developed in [9] whose input is U_R constructed in (5) and its output is Y_R constructed using (14) in step 6.

III. Simulation Results:

A. Methods

To accurately identify a static nonlinearity, it would be ideal to have an input signal that evenly covers its range. The *pseudo random binary sequence* PRBS input which has been extensively used in identification of joint stiffness is far from this ideal.

In this work, we use a pseudo random multilevel position sequence which more effectively covers the velocity input range of the static nonlinearity in the reflex path. Thus, the amplitude distribution of the velocity profile was closer to a uniform distribution. In order to simulate a more realistic environment, we drove our position-servo hydraulic actuator with 100 realizations of this multilevel sequence and recorded its position using a precision potentiometer. These were the inputs used in the simulations.

We also used a realistic model for the additive noise derived from measured experimental data. It had three components: (a) white Gaussian random noise which mimics the measurement noise, (b) Gaussian white noise low-pass filtered at 0.9 Hz to mimic variations in the voluntary torque developed by the subject and (c) a sinusoid which mimics the 60 Hz noise. We scaled the noise sequence to give the appropriate SNR.

We simulated the structure shown in Fig. 1 in MATLAB Simulink. The model was run for 60s at a sampling frequency of 1kHz. We decimated data to 100 Hz for analysis.

We used two nominal models obtained from experimental data. The first had a small reflex contribution, i.e., the cascade gain was small and the threshold of the nonlinearity was large. We used this nominal model to verify the convergence of different methods in identification of the reflex pathway:

$$\begin{aligned} I_1 = 0.014,\ B_1 = 1.645,\ K_1 = 140.810 \\ G_1 = 15.738\ p_1 = 0.604,\ \zeta_1 = 0.412,\ \omega_1 = 8.285 \end{aligned} \tag{15}$$

The second nominal model had a larger reflex response, i.e, the cascade gain was larger and the threshold of the nonlinearity was smaller. We used this nominal model to verify the robustness of different methods as a function of noise level:

$$\begin{aligned} I_2 = 0.015,\ B_2 = 1.507,\ K_2 = 124.454 \\ G_2 = 44.292\ p_2 = 0.161,\ \zeta_2 = 0.576,\ \omega_2 = 11.245 \end{aligned} \tag{16}$$

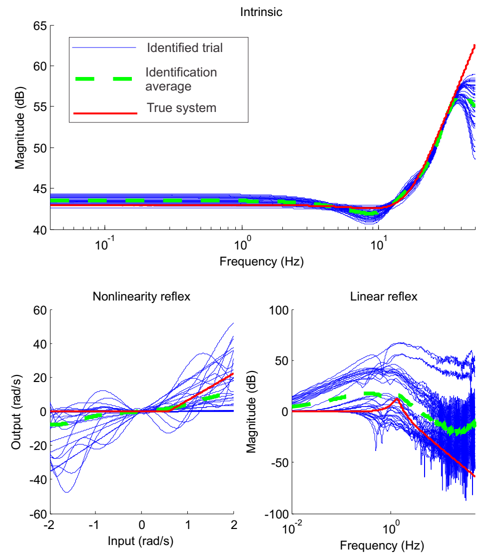

Fig. 2. Identified parallel-cascade models using the parallel-cascade method in a Monte-Carlo simulation of 100 trials, top panel: estimation of the intrinsic stiffness, bottom panel: estimation of the Hammerstein cascade of the reflex stiffness.

B. Results

The first set of Monte Carlo simulations had 100 realizations and used the first nominal model. The objective was to verify convergence of the new subspace and the parallel-cascade methods. Each trial had new realizations of experimental input and noise sequence. Noise was scaled at the output to a SNR of 10dB. We could not use the original (non-iterative) subspace method [8] since it could not identify individual components of the model. For ease of illustration, we present linear systems using their frequency response and show the identified nonlinearities over their input range. We visually verified the accuracy of the identifications by inspecting the bias and variation of the estimates where bias was the difference between the average of the estimates and the true system, and variation was the difference between the individual trial estimates and the average of the estimates.

Fig. 2 shows individual identification trials, identification average and the true system of the parallel-cascade model using the parallel-cascade method [1]. The top panel shows the identified bode diagram of the intrinsic stiffness. It shows that the bias and variation were small. The bottom panels show the estimates of the nonlinearity and linear dynamics of the reflex pathway. Both were badly biased and had large variation. Clearly there were many cases where the method did not converge to the true reflex system.

Fig. 3 shows the models estimated using the new iterative subspace method. It can be seen that the bias and variation of the estimates of both the intrinsic and reflex pathway were much smaller than the parallel-cascade estimates; the average of the estimates was very close to the true system and variation was small. This demonstrates that the subspace method successfully converged and the results were accurate.

In the second set of Monte-Carlo simulations, we used

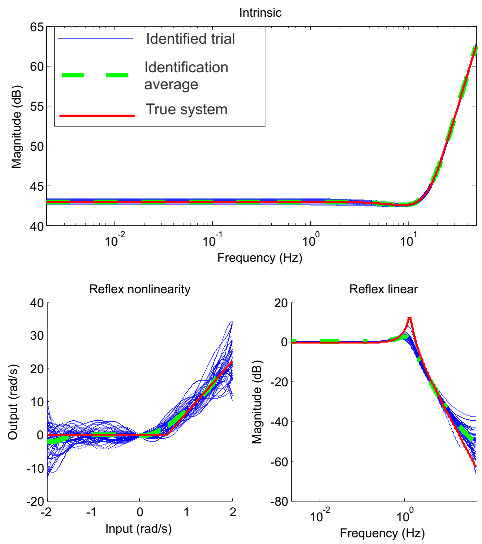

Fig. 3. Identified parallel-cascade models using the new subspace method in a Monte-Carlo simulation of 100 trials, top panel: estimation of the intrinsic stiffness, bottom panel: estimation of the Hammerstein cascade of the reflex stiffness.

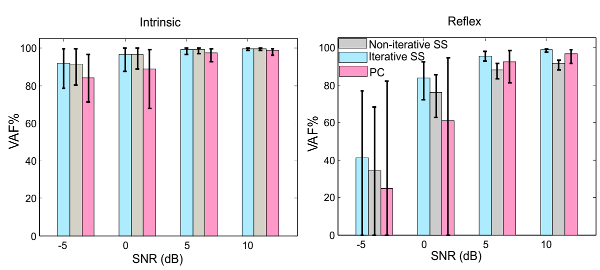

Fig. 4. Intrinsic and reflex mean identification VAF bracketed by 90% range as a function of SNR for three different methods: new iterative subspace, old non-iterative subspace and parallel-cascade.

the second nominal model and systematically changed the SNR level from -5 dB to 10dB. 100 simulations were run at each SNR with different realizations of noise and input. The objective was to demonstrate the robustness of different methods to the noise level in terms of identification *variance accounted for* VAF between the predicted output and the noise-free output. Fig. 4 shows a bar plot at each SNR level showing the mean identification VAF bracketed by its 90% range, i.e. a range that contains 90% of data points.

In identification of the intrinsic pathway, the new method and the non-iterative subspace performed similarly; both accounted for most of the VAF even at the lowest SNR level. Moreover, the mean VAF for both subspace methods was always larger than the parallel-cascade method. In identification of the reflex path, none of the methods provided a reliable estimate at the lowest SNR level. As SNR increased, the new subspace method had larger mean VAFs and smaller variations compared to others, demonstrating that the new subspace method was the most robust to the noise.

IV. Discussion

The contribution of this work is twofold. First, we showed direct estimation of intrinsic mechanics independently of the reflex pathway. This is attractive since the conventional parallel-cascade method needs to iterate between identification of intrinsic and reflex pathways many times before convergence. This approach can be further extended for identification of a system with multiple parallel paths. Thus, each pathway can be independently estimated from others.

Second, we estimate the Hammerstein cascade of the reflex pathway with a state-space structure whose parameters are fewer and directly related to its static nonlinearity and linear component. This is important since makes is straightforward to convert to the continuous time model needed for physiological interpretation.

The proposed approach is iterative but is guaranteed to converge. In general, it is difficult to confirm the convergence of the iterative methods since they need to be initialized in close vicinity of the optimal minimum. The method proposed in this paper is iterative but follows the concept of *normalized alternative convex search* (NACS). The convergence criteria of NACS-based methods have been recently established for any square integrable nonlinearity [11] which does not depend on the choice of initial condition. We can see in Fig. 2 and 3 that the parallel-cascade method failed in most of the trials to converge to the true system presumably because the SNR was large; whereas the new method always converged.

References

[1] R. E. Kearney, R. B. Stein, and L. Parameswaran, "Identification of intrinsic and reflex contributions to human ankle stiffness dynamics," *IEEE Transactions on Biomedical Engineering*, vol. 44, no. 6, pp. 493–504, 1997.

[2] M. Casadio, P. G. Morasso, and V. Sanguineti, "Direct measurement of ankle stiffness during quiet standing: implications for control modelling and clinical application," *Gait & Posture*, vol. 21, no. 4, pp. 410–424, 2005.

[3] D. Westwick and E. J. Perreault, "Closed-loop identification: Application to the estimation of limb impedance in a compliant environment," *IEEE Transactions on Biomedical Engineering*, vol. 58, no. 3, pp. 521–530, 2011.

[4] M. M. Mirbagheri, H. Barbeau, and R. E. Kearney, "Intrinsic and reflex contributions to human ankle stiffness: variation with activation level and position," *Experimental Brain Research*, vol. 135, no. 4, pp. 423–436, 2000.

[5] M. Mirbagheri, H. Barbeau, M. Ladouceur, and R. Kearney, "Intrinsic and reflex stiffness in normal and spastic, spinal cord injured subjects," *Experimental Brain Research*, vol. 141, pp. 446–459, 2001.

[6] D. Ludvig, I. Cathers, and R. Kearney, "Voluntary modulation of human stretch reflexes," *Experimental Brain Research*, vol. 183, pp. 201–213, 2007.

[7] D. Ludvig and R. Kearney, "Estimation of joint stiffness with a compliant load," in *Proceedings of International Conference of the IEEE Engineering in Medicine and Biology Society*, 2009, pp. 2967–2970.

[8] Y. Zhao, D. T. Westwick, and R. E. Kearney, "Subspace methods for identification of human ankle joint stiffness," *IEEE Transactions on Biomedical Engineering*, vol. 58, no. 11, pp. 3039–3048, 2011.

[9] K. Jalaleddini and R. E. Kearney, "An iterative algorithm for the subspace identification of SISO Hammerstein systems," in *Proceedings of IFAC*, 2011, pp. 11 779–11 784.

[10] M. Verhaegen and V. Verdult, *Filtering and System Identification, A Least Squares Approach*. Cambridge University Press, 2007.

[11] G. Q. Li and C. Wen, "Convergence of normalized iterative identification of Hammerstein systems," *Systems & Control Letters*, vol. 60, no. 11, pp. 929–935, 2011.